Eur. Phys. J. C 29, 59–64 (2003)
Digital Object Identifier (DOI) 10.1140/epjc/s2003-01179-3

THE EUROPEAN PHYSICAL JOURNAL C

Unified treatment: analyticity, Regge trajectories, Veneziano amplitude, fundamental regions and Moebius transformations

Abdur Rahim Choudhary[a]

Bell Laboratories, 6426 Grendel Place, Bowie, MD 20720, USA

Received: 22 October 2002 / Revised version: 19 February 2003
Published online: 23 May 2003 – © Springer-Verlag / Società Italiana di Fisica 2003

Abstract. In this paper we present a unified treatment that combines the analyticity properties of the scattering amplitudes, the threshold and asymptotic behaviors, the invariance group of Moebius transformations, the automorphic functions defined over this invariance group, the fundamental region in (Poincaré) geometry, and the generators of the invariance group as they relate to the fundamental region. Using these concepts and techniques, we provide a theoretical basis for Veneziano type amplitudes with the ghost elimination condition built in, related the Regge trajectory functions to the generators of the invariance group, constrained the values of the Regge trajectories to take only inverse integer values at the threshold, used the threshold behavior in the forward direction to deduce the Pomeranchuk trajectory as well as other relations. The enabling tool for this unified treatment came from the multi-sheet conformal mapping techniques that map the physical sheet to a fundamental region which in turn defines a Riemann surface on which a global uniformization variable for the scattering amplitude is calculated via an automorphic function, which in turn can be constructed as a quotient of two automorphic forms of the same dimension.

1 Introduction

Superstring theory, that has evolved into M-theory [1], has its genesis in a representation for the four point scattering amplitude by Veneziano [2]. The Veneziano formula has intrigued the physicists ever since, and a considerable effort has been spent in working backward to understand the underlying principles and symmetries [3,4] (also see [1] and [10]).

The basic physics for our formalism is provided by the analyticity properties [5] of the amplitude $f(s,t)$ in the s-plane, and its threshold and asymptotic behaviors. The approach presented in this paper derives some new relationships that interlink the analyticity properties of the scattering amplitude with a Veneziano type representation for the four-point amplitude and the values of the Regge trajectory functions [6]. We accomplish this by using the multi-sheet conformal mapping techniques [7,8] that unfold the branch points of the scattering amplitude to map its sheets, physical and unphysical, onto a Riemann surface on which the amplitude is a single valued function [9]. The Riemann surface is associated with an automorphic function which affords one to use a global uniformization variable for the expansion of the amplitude on the entire Riemann surface. The automorphic function [19,20] is invariant under a specified group of Moebius transformations, and in our case the group is generated by two generators determined in terms of the values of Regge trajectory functions. The result is a coherent description of many physical aspects in terms of a well-developed mathematical framework. Using this framework we employ conformal mapping techniques to transform the upper half s-plane to a triangle in an ω-plane. The transformation function depends on the variable s and the angles of the triangle. We use arguments based on the behavior of the amplitude at the threshold and asymptotic energies to relate these angles to the values of the Regge trajectory functions. This geometrical picture sheds new light on the Regge trajectory functions, the Veneziano model, the ghost elimination condition, and the Pomeranchuk trajectory. In addition, the formalism has rich mathematical connections to the discontinuous groups of Moebius transformations, fundamental regions, and automorphic functions. We hope that this new picture will provide incentives to the string and membrane theory efforts [10] (see also Chapt. 2 in [1]).

2 Analyticity and conformal mapping

Consider the four point scattering amplitude $f(s,t)$ as a function of the Mandelstam variables [5] s, t, and u with $s+t+u=4m^2$, where m is the mass of each scattering particle in the equal mass case. In this treatment we will take the momentum transfer variable t to be fixed and let s be the energy variable. Such a function has well known analyticity properties as a function of its complex arguments [5]. It has two branch point singularities at $s=s_0$

[a] e-mail: arc@lucent.com

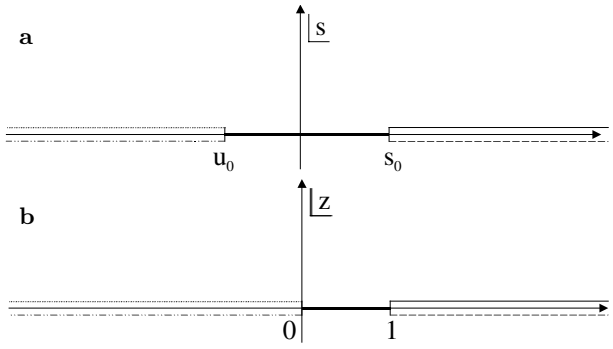

Fig. 1a,b. The analyticity of scattering amplitude in the (a) s-plane, and in the (b) z-plane

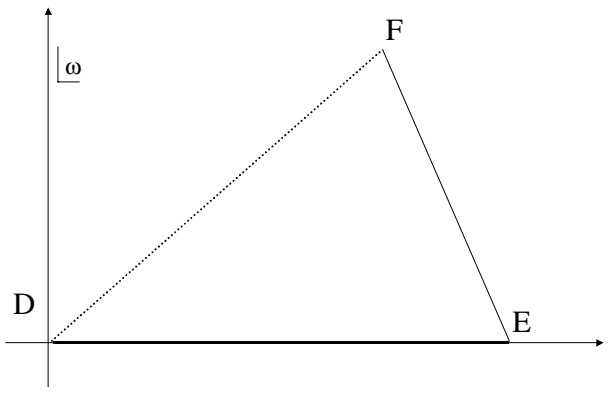

Fig. 2. The upper half z-plane is mapped onto the triangle DEF in the ω-plane

and $s = u_0 \leq 0$ as well as one branch point at ∞. These analyticity properties are shown in Fig. 1a.

The cut along the right hand real s-axis corresponds to the s-channel interactions, while the cut along the negative real s-axis arises from the requirement of crossing symmetry and represents the t-channel interactions [5]. We have considered only the singularities corresponding to the two particle thresholds. These are situated at the branch points s_0 and u_0; if we fix u at $u = u_0$ and let t represent the momentum transfer then the right hand cut starts at $s_0 = 4m^2 - t - u_0$, which takes its lowest value, namely $4m^2$, in the case of forward scattering when $t = 0$ and $u_0 = 0$. For non-forward directions, the point $s_0 = 4m^2$ is an unphysical point and the behavior of the amplitude at this unphysical point is different from the physical threshold behavior, which is known to be of square root type.

We employ a conformal transformation to map the s-plane onto a z-plane such that the three branch points s_0, u_0 and ∞ are respectively mapped onto 1, 0, and ∞:

$$z = \frac{s - u_0}{s_0 - u_0} \; . \tag{1}$$

The cut z-plane is shown in Fig. 1b.

Next we map the upper half cut z-plane ($\mathrm{Im}\, z > 0$) onto the triangle DEF in the ω-plane, as shown in Fig. 2. The existence and construction of this mapping is proven by the Schwarz–Christoffel theorem [11].

The mapping function in the present case is referred to as the Schwarz triangle function, and it is given by the incomplete Euler beta function as follows:

$$\omega(z) = \int_0^z x^{A-1}(1-x)^{B-1}\mathrm{d}x \; . \tag{2}$$

The transformation represented by (2) maps the upper half z-plane onto the triangle DEF such that the branch points at 0, 1, and ∞ in the z-plane are respectively mapped onto the vertices D, E, and F of the triangle DEF in the ω-plane.

The parameters A and B in (2) are related to the interior angles of the triangle DEF as follows:

$$\pi A = \angle\mathrm{EDF} \tag{3a}$$

$$\pi B = \angle\mathrm{DEF} \; . \tag{3b}$$

They determine the precise behavior of the amplitude at its branch points. We now introduce a quantity C as follows:

$$\pi C = \angle\mathrm{DFE} \; . \tag{3c}$$

Obviously we have the following Euclidean relation:

$$A + B + C = 1 \; . \tag{4}$$

3 Relation to Regge trajectories

In order to determine the transformation function ω represented by (2), we need to determine two of the three angles of the triangle DEF. We will do this by requiring that the transformation function ω possess the behavior of the amplitude at the threshold and asymptotic energies. Since the amplitude $f(s,t)$ would eventually be described as a function of ω, it makes sense to build as much of its analyticity as possible into the transformation variable ω. As discussed in [8], this in fact is the main idea behind the multi-Riemann sheet conformal mapping techniques.

For this purpose, let us examine the behavior of the conformal mapping variable ω at the vertices D, E, and F.

3.1 Asymptotic behavior

Let us consider the behavior of (2) for asymptotic values of the energy s. The point $s = \infty$ is mapped onto $z = \infty$, which is mapped onto the vertex F in the ω-plane. In the neighborhood of $z = \infty$, the mapping function ω behaves as follows:

$$\omega(z) = \omega(\infty) + \left[\frac{1}{z} h\left(\frac{1}{z}\right)\right]^{C-1} \; , \tag{5}$$

where C is given by (3c) and $h\left(\frac{1}{z}\right)$ is regular and non-zero at $z = \infty$.

Asymptotically, the amplitude is known to have the Regge behavior [12]

$$f(s,t) \underset{s\to\infty}{\longrightarrow} s^{\alpha(t)} \ , \tag{6}$$

where $\alpha(t)$ is the t-channel Regge trajectory function.

Comparing (5) and (6) and recalling (1) we obtain

$$C = 1 - \alpha(t) \ . \tag{7}$$

The momentum transfer variable $t \leq 0$ is fixed. As t is fixed at different values, the geometry of the triangle in Fig. 2 changes accordingly. This use of a variable geometrical region for the purpose of conformal mapping techniques is one distinguishing aspect of the present research compared to other conformal mapping methods used in particle physics [13].

3.2 Behavior at the branch points

Let us next consider the behavior of (2) at the point s_0. The s-channel threshold s_0 is mapped onto the point $z = 1$ which in turn is mapped onto the vertex E of the triangle. In this neighborhood, the ω of (2) behaves as follows:

$$\omega(z) = \omega(1) + [(z-1)h_1(z-1)]^{B-1} \ , \tag{8}$$

where $h_1(z-1)$ is a function regular and non-zero at $z = 1$, and B is given by (3b).

The behavior of the amplitude at this point is the behavior of the Legendre polynomial $(P_{\alpha(s)}(\cos\theta_s))$ at the branch point $s = s_0$, as it is analytically continued from the point $\alpha(s) = \text{integer}$, $\cos\theta_s = 1 + \frac{2t}{s-s_0}$ to the unphysical point $t \neq 0$, $s = s_0 = 4m^2$. Noting that $\cos\theta \overset{s\to s_0}{\longrightarrow} \infty$ we have [14] (also see [5])

$$f(s,t) \underset{s\to s_0}{\longrightarrow} (s-s_0)^{-\alpha(s_0)} \ , \tag{9}$$

where $\alpha(s)$ is the s-channel Regge trajectory function.

Comparing (8) and (9) and recalling (1) we obtain

$$B = 1 - \alpha(s) \ , \tag{10}$$

where $\alpha(s)$ is evaluated at the branch point $s = s_0$, which is an unphysical point for non-forward directions, i.e. the point s_0 for $t \neq 0$ is unphysical. The behavior of the amplitude in this unphysical region is different from the physical threshold behavior. Equation (9) describes this behavior of the amplitude at the point s_0 in the unphysical region. For the case of forward scattering the point s_0 is the physical threshold and (9) ought to reproduce the known square root type behavior, as we will discuss later.

3.3 Ghost elimination condition

Let us introduce a u-channel Regge trajectory function $\alpha(u)$ as follows:

$$A = 1 - \alpha(u) \ , \tag{11}$$

where A is given by (3a).

Equations (7), (10), and (11) provide a geometrical interpretation for the Regge trajectories. Together with (4), they yield the following relation

$$\alpha(s) + \alpha(t) + \alpha(u) = 2 \ . \tag{12}$$

This is the original condition to eliminate ghosts from the Veneziano amplitude [3]. In our treatment it arises naturally from the formalism whereas in the literature it is imposed by hand. Further, in our formalism the condition arises quite generally.

3.4 Pomeranchuk trajectory and the threshold behavior

The threshold points s_0 and u_0 in Fig. 1a would become the physical two particle thresholds for the case of zero momentum transfer, $t = 0$ and $u_0 = 0$. The branch points at these two particle physical thresholds are of the square root type, as shown in [5]. To obtain a square root behavior at $s = s_0$ we use (8) and (9), and require

$$1 - B = \alpha(s = s_0 = 4m^2) = \tfrac{1}{2} \ . \tag{13}$$

This result is quite general and it arises from the threshold behavior in the forward direction. However such a result for the pion scattering was derived [15] using the Adler zero based on the partially conserved axial vector current (PCAC) approach.

Similarly, for the square root branch point at $s = u_0$, we obtain the following result:

$$1 - A = \alpha(u = u_0 = 0) = \tfrac{1}{2} \ . \tag{14}$$

Invoking (12) we obtain

$$\alpha(t = 0) = 1 \ . \tag{15}$$

This is a Pomeranchuk type trajectory with unit intercept. In our formalism, it arises quite generally from the square root type branch points at the two particle physical thresholds. In view of (6) the Pomeranchuk trajectory will determine the asymptotic behavior, though we have made no recourse to any interpretation of the Pomeranchuk as a Regge pole. The Pomeranchuk trajectory indeed plays an important role in understanding the high energy behavior of total cross sections in the forward direction [16] (also see Chapt. 3 of [5]).

Equation (15) makes no statement on the slope of the Pomeranchuk trajectory. Indeed, it arises from the threshold behavior in the forward direction. Any statement on the slope parameter would, in our formalism, make a simultaneous statement about the threshold behavior in non-forward directions, as one analytically continues from $t = 0$ to the appropriate non-zero t value and the points at which (13) and (14) are evaluated move from the physical region to the unphysical region. This is an interesting and potentially useful relationship, as the experimental data leave an uncertainty in the slope parameter [17]. To restate

the relationship, one must also examine the threshold behavior in the non-forward directions in order to analyze the slope of the Pomeranchuk.

Equations (13)–(15) show that, in the special case of $t = 0$, the triangle in Fig. 2 degenerates into a vertical strip such that the angles at the vertices D and E are each a right angle and the angle at the vertex F is zero. At the same time the mapping function given by (2) reduces to the following trigonometric function:

$$\omega_1(z) = \int_0^z x^{\frac{1}{2}-1}(1-x)^{\frac{1}{2}-1}\mathrm{d}x = \arccos(1-2z) \ . \quad (16)$$

This representation does indeed have the square root type branch points at $z = 1$ and 0, while it behaves logarithmically at infinity. It can be potentially useful to analyze the scattering data in the forward direction. A similar geometry with a different type of branch points did prove useful in the analysis of the partial wave scattering [18].

4 Amplitude representation

As discussed above, the conformal mapping of the upper half s-plane onto the triangle DEF in the ω-plane is given by the following representation:

$$\omega(z) = \int_0^z x^{-\alpha(u)}(1-x)^{-\alpha(s)}\mathrm{d}x \ , \quad (17)$$

where we have substituted (10) and (11) in (2).

As is discussed in [9,25] the value of the conformal mapping variable ω lies in its ability to yield simple representations for the amplitude $f(s,t)$. As a function of ω the amplitude is a meromorphic function, and away from any pole we can seek a representation by the following equation:

$$f(s,t) = \phi(\omega) = \sum_{n=0}^{n=\infty} a_n(\omega - \omega_c)^n \ , \quad (18)$$

where ω is given by (17), and ω_c is the point around which the expansion is sought. This representation can form the basis for polynomial approximations to evaluate the amplitude in special phenomenological cases. Reference [13] describes some examples of such polynomial approximations. Such polynomial approximations will automatically have the correct threshold and asymptotic behavior, and they will reflect the correct analyticity properties of the amplitude with respect to the left and right hand cuts involving the three branch point singularities shown in Fig. 1. Below, we illustrate this point by seeking the simplest approximations around the three vertices of the triangle DEF in Fig. 2.

For the approximation near the vertex D, we recall that the variable ω correctly represents the analyticity of the amplitude, i.e. it carries the two particle thresholds for the s- and t-channels, as well as the threshold and asymptotic behaviors. Taking $\omega_c = 0$ in (18) the simplest representation for the amplitude is as follows:

$$\phi_0(\omega) = \omega \ . \quad (19)$$

For the approximation near the vertex E, which corresponds to $s = s_0$ or $z = 1$, we use (19) to evaluate the constant term in (18) for the expansion around the s-channel threshold. This constant term reads as follows:

$$\frac{\Gamma(1-\alpha(s))\Gamma(1-\alpha(u))}{\Gamma(2-\alpha(s)-\alpha(u))} \ . \quad (20)$$

For the approximation near the vertex F, let us expand about the point at infinity, which corresponds to $z = \infty$. A similar procedure yields the constant term for this expansion as follows:

$$\frac{\Gamma(1-\alpha(s))\Gamma(1-\alpha(u))}{\Gamma(2-\alpha(s)-\alpha(u))} + (-1)^{-\alpha(s)}\frac{\Gamma(1-\alpha(s))\Gamma(1-\alpha(t))}{\Gamma(2-\alpha(s)-\alpha(t))} \ , \quad (21)$$

where we decomposed the range of integration 0 to ∞ into the ranges 0 to 1 and 1 to ∞, changed the variable as $z \to \frac{1}{r}$ in the second range, and used (12).

The similarity of these terms with the Veneziano model is obvious. The next order terms can also be included, which may help to restore the unitarity property of the Veneziano amplitude, in so far as they incorporate the branch point cuts.

Equations (20) and (21) would correspond to the Veneziano model under two ad hoc assumptions. First, one has to assume that the Regge trajectory functions can be meaningfully defined away from the point at which (20) and (21) are evaluated. Second, one has to postulate that when the trajectory functions are so defined, the higher order terms in (18) can be neglected. Our formalism provides a systematic way to scrutinize such assumptions and possibly can help resolve some problems, such as the violation of unitarity.

The representations given in this section hold for the Regge trajectories that are used to evaluate (3a) through (3c) in the light of the relations (7), (10), and (11).

5 Relationship to automorphic functions

Let us take another look at Fig. 2. It shows how the upper half z-plane shown in Fig. 1b is mapped onto the ω-plane. Let us now consider how the entire z-plane maps onto the ω-plane. This is shown in Fig. 3. The entire z-plane in Fig. 1b is mapped on to the quadrilateral DFEG in the ω-plane by the transformation in (2), and equivalently (17). The upper and lower edges of the right hand cut in Fig. 1 have been unfolded onto the sides EF and EG respectively, of the quadrilateral DFEG, and they are called conjugate sides. Similarly, the upper and lower edges of the left hand cut have been unfolded onto the conjugate sides DF and DG respectively.

In the parlance of automorphic functions and discontinuous groups of Moebius transformations [19,20], the quadrilateral DFEG is referred to as a "fundamental region". There is a group of discontinuous transformations

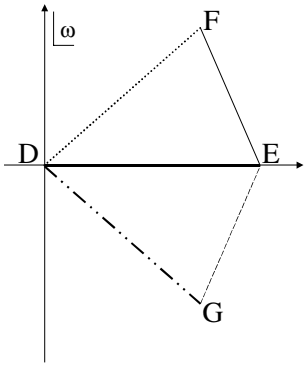

Fig. 3. Mapping of the entire z-plane shown in Fig. 1b on to the ω-plane

associated with this fundamental region. The group is generated by the transformations that map the pair of conjugate sides of the fundamental region onto each other. Thus one generator of the group is the transformation that maps the side DF on the side DG. It is given by the rotation represented by the Moebius transformation T_1 below:

$$T_1 = \begin{pmatrix} \exp(-\mathrm{i}\pi\alpha(u)) & 0 \\ 0 & \exp(\mathrm{i}\pi\alpha(u)) \end{pmatrix} . \tag{22}$$

The second generator corresponds to the transformation that maps the side EF on the side EG. It is given by the Moebius transformation T_2 below:

$$T_2 = \begin{pmatrix} \exp(\mathrm{i}\pi\alpha(s)) & (2\mathrm{i}d)\sin\pi\alpha(s) \\ 0 & \exp(-\mathrm{i}\pi\alpha(s)) \end{pmatrix} , \tag{23}$$

where d is the length DE in Fig. 3, which is represented by the expression numbered (20) above. Thus d is given by the following equation:

$$d = \frac{\Gamma(1-\alpha(s))\Gamma(1-\alpha(u))}{\Gamma(2-\alpha(s)-\alpha(u))} . \tag{24}$$

It is interesting that the values of the Regge trajectory functions enter in the generators for the underlying invariance group.

Each copy of the fundamental region DFEG under a Moebius transformation belonging to the group generated by the above generators is a complete map of the entire z-plane. The conformal mapping variable ω is thus a multivalued function of z. The inverse transformation of (2), or equivalently (17), would map the multiple values of ω on to the same value of z, and z is an automorphic function of ω under the group of discontinous transformations generated by T_1 and T_2. The automorphic functions are a strong instrument to understand some interrelations between geometry, discrete groups of Moebius transformations, and conformal mappings [8].

At the same time, according to a theorem, the transforms of the "fundamental region" under these transformations will completely cover the ω-plane, without overlaps and without leaving any chinks [19,20]. This aspect requires that the generators T_1 and T_2 be cyclic of finite or infinite order. If a generator would have a finite order n, it implies from the structure of T_1 and T_2 that the corresponding Regge trajectory function shall take values at the threshold points s_0 and u_0 according to the following constraint:

$$\alpha = \frac{1}{n} . \tag{25}$$

Two special cases of this result were described above. One corresponds to $n = 1$ which corresponds to (15) for the Pomeranchuk trajectory. The case $n = 2$ corresponds to (14) that also corresponds to the Adler zero.

Equation (25) has another significance. Without such a constraint, the group of transformations generated by the generators in (22) and (23) might not be a subgroup of the modular group. The relevance of the subgroups of the modular group in reproducing the mass spectrum of the particles was realized [21] early in the history of the dual strings.

6 Generalization to non-Euclidean geometry

The approach can be extended to the case of non-Euclidean geometry, in particular the Poincaré model [22]. The need to use non-Euclidean geometry would be indicated if the constraint in (12) would read as follows:

$$\alpha(s) + \alpha(t) + \alpha(u) > 2 . \tag{26}$$

This can correspond to the case where the generators of the underlying discontinuous group of Moebius transformations would turn out to be cyclic with infinite order. The geometry for the fundamental region would then involve curvilinear triangles. The transformation would then be represented by a general class of functions known as Riemann–Schwarz triangle functions [23]. Defining A, B, and C as in (3a) to (3c), the relationship between the angles now reads as follows:

$$A + B + C < 1 . \tag{27}$$

The transformation from the z-plane to the ω-plane is now given by the following equation:

$$\omega = \tau(z) = \frac{f_1(z)}{f_2(z)} , \tag{28}$$

where

$$f_1(z) = \int_0^1 \mathrm{d}t \left[t^{-\frac{1}{2}(1+A+B+C)} (1-t)^{-\frac{1}{2}(1+A-B-C)} (1-zt)^{-\frac{1}{2}(1-A+B-C)} \right] , \tag{29a}$$

$$f_2(z) = \int_0^1 \mathrm{d}t \left[t^{-\frac{1}{2}(1+A+B+C)} (1-t)^{-\frac{1}{2}(1-A-B+C)} (1-t+zt)^{-\frac{1}{2}(1-A+B-C)} \right] . \tag{29b}$$

An alternative representation using the familiar Gamma functions (Γ) and Gaussian hypergeometric functions (${}_2^{}F_1^{}$) is as follows:

$$\tau(z) = \frac{g_1(z)}{g_2(z)}\,, \tag{30}$$

where

$$g_1(z) = \frac{\Gamma\left(\frac{1}{2}(1-A+B+C)\right)}{\Gamma(1-A)} \times {}_2^{}F_1^{}\left(\tfrac{1}{2}(1-A+B-C), \tfrac{1}{2}(1-A-B-C); 1-A; z\right)\,, \tag{31a}$$

$$g_2(z) = \frac{\Gamma\left(\frac{1}{2}(1+A+B-C)\right)}{\Gamma(1-C)} \times {}_2^{}F_1^{}\left(\tfrac{1}{2}(1-A+B-C), \tfrac{1}{2}(1-A-B-C); 1-C; 1-z\right)\,. \tag{31b}$$

A special case corresponding to $A = B = C = 0$ of this transformation was found to be useful in exploring the analyticity properties of the partial wave scattering amplitudes [24]. The result was a generalized effective range theory that was valid for all non-relativistic energies and offered a fast convergence rate [25].

7 Summary and conclusions

In this paper we used the basic physical input in the form of the analyticity of the scattering amplitude, its asymptotic behavior, and its behavior at the branch points. We used the tools provided by the multi-sheet conformal mapping techniques to derive numerous inter-relationships; some previously known in the literature, though from quite a different theoretical basis, and some new ones. The formalism yielded many significant results: it related the Veneziano type amplitude to the analyticity; it provided a theoretical basis for the ghost elimination condition as well as possible approaches to restore unitarity. Additional relationships are also derived, including the existence of a Pomeranchuk type trajectory with a unit intercept. The Pomeranchuk is expected as a consequence of the square root type behavior at the two particle thresholds for the forward scattering. It is also expected via the constraint (25) on the values of the Regge trajectory functions. This constraint derives from a new relationship that our formalism makes possible by connecting the Regge trajectory functions to the generators of the underlying invariance group of discontinuous transformations. The formalism relates the slope parameter of the Pomeranchuk trajectory to the analytic continuation of the forward scattering amplitude to the non-forward directions in the vicinity of the two particle thresholds. Further consequences of these new relationships remain to be explored.

Acknowledgements. I would like to dedicate this work to my mother Khadijah Begum (1921–2001), and to my father Choudhary Ali Mohammad (1918–1974).

References

1. M. Kaku, in Introduction to superstrings and M-theory, second edition (Springer, 1999)
2. G. Veneziano, Nuovo Cimento A **57**, 190 (1968)
3. D. Fairlie, Nucl. Phys. B **433**, 26 (1995)
4. R. Fiore, L.L. Jenkovszky, V. Magas, F. Paccanoni, A. Papa, DFPD 00/TH/50 and UNICAL-TH 00/8 (2000)
5. R.J. Eden, P.V. Landshoff, D.I. Olive, J.C. Polkinghorne, in The analytic S-matrix (Cambridge University Press, 1966)
6. A.E. Inopin, hep-ph/0110160 (2001). (Submitted to Int. J. Mod. Phys. A)
7. H. Kober, in Dictionary of conformal representations, 2nd edition (Dover Publications, New York 1957)
8. A.R. Choudhary, R.B. Jones, J. Phys. A **5**, 981 (1972)
9. R.B. Jones, Commun. Math. Phys. **17**, 143 (1970)
10. M. Kaku, in Strings, Conformal Fields, and M-Theory, second edition (Springer, 2000)
11. L.V. Ahlfors, in Complex analysis, 2nd edition (McGraw Hill, 1966)
12. S.C. Frautschi, in Regge poles and S-matrix theory (Benjamin, New York, 1963)
13. W. Langbein, Nuovo Cimento A **39**, 313 (1977)
14. R. Omnes, Introduction to particle physics, Chapter 14 on Regge Poles (Wiley-Interscience, 1970)
15. C. Lovelace, Phys. Lett. B **28**, 264 (1968)
16. J.R. Cudell, V. Ezhela, K. Kang, S. Lugovsky, N. Tkachenko, Phys. Rev. D **61**, 034019 (2000)
17. P. Desgrolard, E. Martinov, hep-ph/010277 (2001)
18. A.R. Choudhary, Phys. Rev. C **27**, 398 (1983)
19. L.R. Ford, in Automorphic functions (Chelsea, New York 1951)
20. J. Lehner, in Discontinuous groups and automorphic functions, Mathematical Surveys No. VIII (Amer. Math. Soc., 1964)
21. W. Nahm, Nucl. Phys. B **114**, 174 (1976)
22. S. Stahl, in The Poincaré half plane: a gateway to modern geometry (Jones and Bartlett, Boston 1993)
23. A. Erdelyi, in Higher tanscendental functions, Vol. 1, p. 96 and Vol. 3, p. 33 (McGraw Hill, 1953)
24. A.R. Choudhary, R.B. Jones, Nucl. Phys. B **22**, 343 (1970)
25. A.R. Choudhary, Nuovo Cimento A **24**, 161 (1974)